

Search for a resonance decaying into WZ boson pairs in $p\bar{p}$ collisions

V.M. Abazov³⁷, B. Abbott⁷⁵, M. Abolins⁶⁵, B.S. Acharya³⁰, M. Adams⁵¹, T. Adams⁴⁹, E. Aguilo⁶, M. Ahsan⁵⁹, G.D. Alexeev³⁷, G. Alkhazov⁴¹, A. Alton^{64,a}, G. Alverson⁶³, G.A. Alves², L.S. Ancu³⁶, M. Aoki⁵⁰, Y. Arnaud¹⁴, M. Arov⁶⁰, A. Askew⁴⁹, B. Åsman⁴², O. Atramentov^{49,b}, C. Avila⁸, J. BackusMayes⁸², F. Badaud¹³, L. Bagby⁵⁰, B. Baldin⁵⁰, D.V. Bandurin⁵⁹, S. Banerjee³⁰, E. Barberis⁶³, A.-F. Barfuss¹⁵, P. Baringer⁵⁸, J. Barreto², J.F. Bartlett⁵⁰, U. Bassler¹⁸, D. Bauer⁴⁴, S. Beale⁶, A. Bean⁵⁸, M. Begalli³, M. Begel⁷³, C. Belanger-Champagne⁴², L. Bellantoni⁵⁰, J.A. Benitez⁶⁵, S.B. Beri²⁸, G. Bernardi¹⁷, R. Bernhard²³, I. Bertram⁴³, M. Besançon¹⁸, R. Beuselinck⁴⁴, V.A. Bezzubov⁴⁰, P.C. Bhat⁵⁰, V. Bhatnagar²⁸, G. Blazey⁵², S. Blessing⁴⁹, K. Bloom⁶⁷, A. Boehnlein⁵⁰, D. Boline⁶², T.A. Bolton⁵⁹, E.E. Boos³⁹, G. Borissov⁴³, T. Bose⁶², A. Brandt⁷⁸, R. Brock⁶⁵, G. Brooijmans⁷⁰, A. Bross⁵⁰, D. Brown¹⁹, X.B. Bu⁷, D. Buchholz⁵³, M. Buehler⁸¹, V. Buescher²⁵, V. Bunichev³⁹, S. Burdin^{43,c}, T.H. Burnett⁸², C.P. Buszello⁴⁴, P. Calfayan²⁶, B. Calpas¹⁵, S. Calvet¹⁶, E. Camacho-Pérez³⁴, J. Cammin⁷¹, M.A. Carrasco-Lizarraga³⁴, E. Carrera⁴⁹, W. Carvalho³, B.C.K. Casey⁵⁰, H. Castilla-Valdez³⁴, S. Chakrabarti⁷², D. Chakraborty⁵², K.M. Chan⁵⁵, A. Chandra⁵⁴, E. Cheu⁴⁶, S. Chevalier-Théry¹⁸, D.K. Cho⁶², S.W. Cho³², S. Choi³³, B. Choudhary²⁹, T. Christoudias⁴⁴, S. Cihangir⁵⁰, D. Claes⁶⁷, J. Clutter⁵⁸, M. Cooke⁵⁰, W.E. Cooper⁵⁰, M. Corcoran⁸⁰, F. Couderc¹⁸, M.-C. Cousinou¹⁵, D. Cutts⁷⁷, M. Ćwiok³¹, A. Das⁴⁶, G. Davies⁴⁴, K. De⁷⁸, S.J. de Jong³⁶, E. De La Cruz-Burelo³⁴, K. DeVaughan⁶⁷, F. Déliot¹⁸, M. Demarteau⁵⁰, R. Demina⁷¹, D. Denisov⁵⁰, S.P. Denisov⁴⁰, S. Desai⁵⁰, H.T. Diehl⁵⁰, M. Diesburg⁵⁰, A. Dominguez⁶⁷, T. Dorland⁸², A. Dubey²⁹, L.V. Dudko³⁹, L. Dufлот¹⁶, D. Duggan⁴⁹, A. Duperrin¹⁵, S. Dutt²⁸, A. Dyshkant⁵², M. Eads⁶⁷, D. Edmunds⁶⁵, J. Ellison⁴⁸, V.D. Elvira⁵⁰, Y. Enari¹⁷, S. Eno⁶¹, H. Evans⁵⁴, A. Evdokimov⁷³, V.N. Evdokimov⁴⁰, G. Facini⁶³, A.V. Ferapontov⁷⁷, T. Ferbel^{61,71}, F. Fiedler²⁵, F. Filthaut³⁶, W. Fisher⁵⁰, H.E. Fisk⁵⁰, M. Fortner⁵², H. Fox⁴³, S. Fuess⁵⁰, T. Gadfort⁷⁰, C.F. Galea³⁶, A. Garcia-Bellido⁷¹, V. Gavrilov³⁸, P. Gay¹³, W. Geist¹⁹, W. Geng^{15,65}, D. Gerbaudo⁶⁸, C.E. Gerber⁵¹, Y. Gershtein^{49,b}, D. Gillberg⁶, G. Ginther^{50,71}, G. Golovanov³⁷, B. Gómez⁸, A. Goussiou⁸², P.D. Grannis⁷², S. Greder¹⁹, H. Greenlee⁵⁰, Z.D. Greenwood⁶⁰, E.M. Gregores⁴, G. Grenier²⁰, Ph. Gris¹³, J.-F. Grivaz¹⁶, A. Grohsjean¹⁸, S. Grünendahl⁵⁰, M.W. Grünewald³¹, F. Guo⁷², J. Guo⁷², G. Gutierrez⁵⁰, P. Gutierrez⁷⁵, A. Haas^{70,d}, P. Haefner²⁶, S. Hagopian⁴⁹, J. Haley⁶³, I. Hall⁶⁵, R.E. Hall⁴⁷, L. Han⁷, K. Harder⁴⁵, A. Harel⁷¹, J.M. Hauptman⁵⁷, J. Hays⁴⁴, T. Hebbeker²¹, D. Hedin⁵², J.G. Hegeman³⁵, A.P. Heinson⁴⁸, U. Heintz⁶², C. Hensel²⁴, I. Heredia-De La Cruz³⁴, K. Herner⁶⁴, G. Hesketh⁶³, M.D. Hildreth⁵⁵, R. Hirsch⁸¹, T. Hoang⁴⁹, J.D. Hobbs⁷², B. Hoeneisen¹², M. Hohlfeld²⁵, S. Hossain⁷⁵, P. Houben³⁵, Y. Hu⁷², Z. Hubacek¹⁰, N. Huske¹⁷, V. Hynek¹⁰, I. Iashvili⁶⁹, R. Illingworth⁵⁰, A.S. Ito⁵⁰, S. Jabeen⁶², M. Jaffré¹⁶, S. Jain⁷⁵, K. Jakobs²³, D. Jamin¹⁵, R. Jesik⁴⁴, K. Johns⁴⁶, C. Johnson⁷⁰, M. Johnson⁵⁰, D. Johnston⁶⁷, A. Jonckheere⁵⁰, P. Jonsson⁴⁴, A. Juste⁵⁰, K. Kaadze⁵⁹, E. Kajfasz¹⁵, D. Karmanov³⁹, P.A. Kasper⁵⁰, I. Katsanos⁶⁷, V. Kaushik⁷⁸, R. Kehoe⁷⁹, S. Kermiche¹⁵, N. Khalatyan⁵⁰, A. Khanov⁷⁶, A. Kharchilava⁶⁹, Y.N. Kharzhev³⁷, D. Khatidze⁷⁷, M.H. Kirby⁵³, M. Kirsch²¹, J.M. Kohli²⁸, A.V. Kozelov⁴⁰, J. Kraus⁶⁵, A. Kumar⁶⁹, A. Kupco¹¹, T. Kurča²⁰, V.A. Kuzmin³⁹, J. Kvita⁹, F. Lacroix¹³, D. Lam⁵⁵, S. Lammers⁵⁴, G. Landsberg⁷⁷, P. Lebrun²⁰, H.S. Lee³², W.M. Lee⁵⁰, A. Leflat³⁹, J. Lellouch¹⁷, L. Li⁴⁸, Q.Z. Li⁵⁰, S.M. Lietti⁵, J.K. Lim³², D. Lincoln⁵⁰, J. Linnemann⁶⁵, V.V. Lipaev⁴⁰, R. Lipton⁵⁰, Y. Liu⁷, Z. Liu⁶, A. Lobodenko⁴¹, M. Lokajicek¹¹, P. Love⁴³, H.J. Lubatti⁸², R. Luna-Garcia^{34,e}, A.L. Lyon⁵⁰, A.K.A. Maciel², D. Mackin⁸⁰, P. Mättig²⁷, R. Magaña-Villalba³⁴, P.K. Mal⁴⁶, S. Malik⁶⁷, V.L. Malyshev³⁷, Y. Maravin⁵⁹, B. Martin¹⁴, J. Martínez-Ortega³⁴, R. McCarthy⁷², C.L. McGivern⁵⁸, M.M. Meijer³⁶, A. Melnitchouk⁶⁶, L. Mendoza⁸, D. Menezes⁵², P.G. Mercadante⁴, M. Merkin³⁹, A. Meyer²¹, J. Meyer²⁴, N.K. Mondal³⁰, R.W. Moore⁶, T. Moulik⁵⁸, G.S. Muanza¹⁵, M. Mulhearn⁸¹, O. Mundal²², L. Mundim³, E. Nagy¹⁵, M. Naimuddin²⁹, M. Narain⁷⁷, R. Nayyar²⁹, H.A. Neal⁶⁴, J.P. Negret⁸, P. Neustroev⁴¹, H. Nilsen²³, H. Nogima³, S.F. Novaes⁵, T. Nunnemann²⁶, G. Obrant⁴¹, D. Onoprienko⁵⁹, J. Orduna³⁴, N. Osman⁴⁴, J. Osta⁵⁵, R. Otec¹⁰, G.J. Otero y Garzón¹, M. Owen⁴⁵, M. Padilla⁴⁸, P. Padley⁸⁰, M. Pangilinan⁷⁷, N. Parashar⁵⁶, V. Parihar⁶², S.-J. Park²⁴, S.K. Park³², J. Parsons⁷⁰, R. Partridge⁷⁷, N. Parua⁵⁴, A. Patwa⁷³, B. Penning⁵⁰, M. Perfilov³⁹, K. Peters⁴⁵, Y. Peters⁴⁵, P. Pétrouff¹⁶, R. Piegaia¹, J. Piper⁶⁵, M.-A. Pleier⁷³, P.L.M. Podesta-Lerma^{34,f}, V.M. Podstavkov⁵⁰, Y. Pogorelov⁵⁵, M.-E. Pol², P. Polozov³⁸, A.V. Popov⁴⁰, M. Prewitt⁸⁰, S. Protopopescu⁷³, J. Qian⁶⁴, A. Quadt²⁴, B. Quinn⁶⁶, M.S. Rangel¹⁶, K. Ranjan²⁹, P.N. Ratoff⁴³, I. Razumov⁴⁰, P. Renkel⁷⁹, P. Rich⁴⁵, M. Rijssenbeek⁷², I. Ripp-Baudot¹⁹, F. Rizatdinova⁷⁶, S. Robinson⁴⁴, M. Rominsky⁷⁵, C. Royon¹⁸, P. Rubinov⁵⁰, R. Ruchti⁵⁵, G. Safronov³⁸, G. Sajot¹⁴, A. Sánchez-Hernández³⁴, M.P. Sanders²⁶, B. Sanghi⁵⁰, G. Savage⁵⁰,

L. Sawyer⁶⁰, T. Scanlon⁴⁴, D. Schaile²⁶, R.D. Schamberger⁷², Y. Scheglov⁴¹, H. Schellman⁵³, T. Schliephake²⁷, S. Schlobohm⁸², C. Schwanenberger⁴⁵, R. Schwienhorst⁶⁵, J. Sekaric⁵⁸, H. Severini⁷⁵, E. Shabalina²⁴, M. Shamim⁵⁹, V. Shary¹⁸, A.A. Shchukin⁴⁰, R.K. Shivpuri²⁹, V. Simak¹⁰, V. Sirotenko⁵⁰, P. Skubic⁷⁵, P. Slattery⁷¹, D. Smirnov⁵⁵, G.R. Snow⁶⁷, J. Snow⁷⁴, S. Snyder⁷³, S. Söldner-Rembold⁴⁵, L. Sonnenschein²¹, A. Sopczak⁴³, M. Sosebee⁷⁸, K. Soustruznik⁹, B. Spurlock⁷⁸, J. Stark¹⁴, V. Stolin³⁸, D.A. Stoyanova⁴⁰, J. Strandberg⁶⁴, M.A. Strang⁶⁹, E. Strauss⁷², M. Strauss⁷⁵, R. Ströhmer²⁶, D. Strom⁵¹, L. Stutte⁵⁰, S. Sumowidagdo⁴⁹, P. Svoisky³⁶, M. Takahashi⁴⁵, A. Tanasijczuk¹, W. Taylor⁶, B. Tiller²⁶, M. Titov¹⁸, V.V. Tokmenin³⁷, I. Torchiani²³, D. Tsybychev⁷², B. Tuchming¹⁸, C. Tully⁶⁸, P.M. Tuts⁷⁰, R. Unalan⁶⁵, L. Uvarov⁴¹, S. Uvarov⁴¹, S. Uzunyan⁵², P.J. van den Berg³⁵, R. Van Kooten⁵⁴, W.M. van Leeuwen³⁵, N. Varelas⁵¹, E.W. Varnes⁴⁶, I.A. Vasilyev⁴⁰, P. Verdier²⁰, L.S. Vertogradov³⁷, M. Verzocchi⁵⁰, M. Vesterinen⁴⁵, D. Vilanova¹⁸, P. Vint⁴⁴, P. Vokac¹⁰, R. Wagner⁶⁸, H.D. Wahl⁴⁹, M.H.L.S. Wang⁷¹, J. Warchol⁵⁵, G. Watts⁸², M. Wayne⁵⁵, G. Weber²⁵, M. Weber^{50,g}, A. Wenger^{23,h}, M. Wetstein⁶¹, A. White⁷⁸, D. Wicke²⁵, M.R.J. Williams⁴³, G.W. Wilson⁵⁸, S.J. Wimpenny⁴⁸, M. Wobisch⁶⁰, D.R. Wood⁶³, T.R. Wyatt⁴⁵, Y. Xie⁷⁷, C. Xu⁶⁴, S. Yacoub⁵³, R. Yamada⁵⁰, W.-C. Yang⁴⁵, T. Yasuda⁵⁰, Y.A. Yatsunenkov³⁷, Z. Ye⁵⁰, H. Yin⁷, K. Yip⁷³, H.D. Yoo⁷⁷, S.W. Youn⁵⁰, J. Yu⁷⁸, C. Zeitnitz²⁷, S. Zelitch⁸¹, T. Zhao⁸², B. Zhou⁶⁴, J. Zhu⁷², M. Zielinski⁷¹, D. Zieminska⁵⁴, L. Zivkovic⁷⁰, V. Zutshi⁵², and E.G. Zverev³⁹

(The DØ Collaboration)

¹Universidad de Buenos Aires, Buenos Aires, Argentina

²LAFEX, Centro Brasileiro de Pesquisas Físicas, Rio de Janeiro, Brazil

³Universidade do Estado do Rio de Janeiro, Rio de Janeiro, Brazil

⁴Universidade Federal do ABC, Santo André, Brazil

⁵Instituto de Física Teórica, Universidade Estadual Paulista, São Paulo, Brazil

⁶University of Alberta, Edmonton, Alberta, Canada; Simon Fraser University, Burnaby, British Columbia, Canada; York University, Toronto, Ontario, Canada and McGill University, Montreal, Quebec, Canada

⁷University of Science and Technology of China, Hefei, People's Republic of China

⁸Universidad de los Andes, Bogotá, Colombia

⁹Center for Particle Physics, Charles University,

Faculty of Mathematics and Physics, Prague, Czech Republic

¹⁰Czech Technical University in Prague, Prague, Czech Republic

¹¹Center for Particle Physics, Institute of Physics,

Academy of Sciences of the Czech Republic, Prague, Czech Republic

¹²Universidad San Francisco de Quito, Quito, Ecuador

¹³LPC, Université Blaise Pascal, CNRS/IN2P3, Clermont, France

¹⁴LPSC, Université Joseph Fourier Grenoble 1, CNRS/IN2P3,

Institut National Polytechnique de Grenoble, Grenoble, France

¹⁵CPPM, Aix-Marseille Université, CNRS/IN2P3, Marseille, France

¹⁶LAL, Université Paris-Sud, IN2P3/CNRS, Orsay, France

¹⁷LPNHE, IN2P3/CNRS, Universités Paris VI and VII, Paris, France

¹⁸CEA, Irfu, SPP, Saclay, France

¹⁹IPHC, Université de Strasbourg, CNRS/IN2P3, Strasbourg, France

²⁰IPNL, Université Lyon 1, CNRS/IN2P3, Villeurbanne, France and Université de Lyon, Lyon, France

²¹III. Physikalisches Institut A, RWTH Aachen University, Aachen, Germany

²²Physikalisches Institut, Universität Bonn, Bonn, Germany

²³Physikalisches Institut, Universität Freiburg, Freiburg, Germany

²⁴II. Physikalisches Institut, Georg-August-Universität Göttingen, Göttingen, Germany

²⁵Institut für Physik, Universität Mainz, Mainz, Germany

²⁶Ludwig-Maximilians-Universität München, München, Germany

²⁷Fachbereich Physik, University of Wuppertal, Wuppertal, Germany

²⁸Panjab University, Chandigarh, India

²⁹Delhi University, Delhi, India

³⁰Tata Institute of Fundamental Research, Mumbai, India

³¹University College Dublin, Dublin, Ireland

³²Korea Detector Laboratory, Korea University, Seoul, Korea

³³SungKyunKwan University, Suwon, Korea

³⁴CINVESTAV, Mexico City, Mexico

³⁵FOM-Institute NIKHEF and University of Amsterdam/NIKHEF, Amsterdam, The Netherlands

³⁶Radboud University Nijmegen/NIKHEF, Nijmegen, The Netherlands

³⁷Joint Institute for Nuclear Research, Dubna, Russia

³⁸Institute for Theoretical and Experimental Physics, Moscow, Russia

- ³⁹*Moscow State University, Moscow, Russia*
⁴⁰*Institute for High Energy Physics, Protvino, Russia*
⁴¹*Petersburg Nuclear Physics Institute, St. Petersburg, Russia*
⁴²*Stockholm University, Stockholm, Sweden, and Uppsala University, Uppsala, Sweden*
⁴³*Lancaster University, Lancaster, United Kingdom*
⁴⁴*Imperial College London, London SW7 2AZ, United Kingdom*
⁴⁵*The University of Manchester, Manchester M13 9PL, United Kingdom*
⁴⁶*University of Arizona, Tucson, Arizona 85721, USA*
⁴⁷*California State University, Fresno, California 93740, USA*
⁴⁸*University of California, Riverside, California 92521, USA*
⁴⁹*Florida State University, Tallahassee, Florida 32306, USA*
⁵⁰*Fermi National Accelerator Laboratory, Batavia, Illinois 60510, USA*
⁵¹*University of Illinois at Chicago, Chicago, Illinois 60607, USA*
⁵²*Northern Illinois University, DeKalb, Illinois 60115, USA*
⁵³*Northwestern University, Evanston, Illinois 60208, USA*
⁵⁴*Indiana University, Bloomington, Indiana 47405, USA*
⁵⁵*University of Notre Dame, Notre Dame, Indiana 46556, USA*
⁵⁶*Purdue University Calumet, Hammond, Indiana 46323, USA*
⁵⁷*Iowa State University, Ames, Iowa 50011, USA*
⁵⁸*University of Kansas, Lawrence, Kansas 66045, USA*
⁵⁹*Kansas State University, Manhattan, Kansas 66506, USA*
⁶⁰*Louisiana Tech University, Ruston, Louisiana 71272, USA*
⁶¹*University of Maryland, College Park, Maryland 20742, USA*
⁶²*Boston University, Boston, Massachusetts 02215, USA*
⁶³*Northeastern University, Boston, Massachusetts 02115, USA*
⁶⁴*University of Michigan, Ann Arbor, Michigan 48109, USA*
⁶⁵*Michigan State University, East Lansing, Michigan 48824, USA*
⁶⁶*University of Mississippi, University, Mississippi 38677, USA*
⁶⁷*University of Nebraska, Lincoln, Nebraska 68588, USA*
⁶⁸*Princeton University, Princeton, New Jersey 08544, USA*
⁶⁹*State University of New York, Buffalo, New York 14260, USA*
⁷⁰*Columbia University, New York, New York 10027, USA*
⁷¹*University of Rochester, Rochester, New York 14627, USA*
⁷²*State University of New York, Stony Brook, New York 11794, USA*
⁷³*Brookhaven National Laboratory, Upton, New York 11973, USA*
⁷⁴*Langston University, Langston, Oklahoma 73050, USA*
⁷⁵*University of Oklahoma, Norman, Oklahoma 73019, USA*
⁷⁶*Oklahoma State University, Stillwater, Oklahoma 74078, USA*
⁷⁷*Brown University, Providence, Rhode Island 02912, USA*
⁷⁸*University of Texas, Arlington, Texas 76019, USA*
⁷⁹*Southern Methodist University, Dallas, Texas 75275, USA*
⁸⁰*Rice University, Houston, Texas 77005, USA*
⁸¹*University of Virginia, Charlottesville, Virginia 22901, USA and*
⁸²*University of Washington, Seattle, Washington 98195, USA*

We present the first search for an electrically charged resonance W' decaying to a WZ boson pair using 4.1 fb^{-1} of integrated luminosity collected with the D0 detector at the Fermilab Tevatron $p\bar{p}$ collider. The WZ pairs are reconstructed through their decays into three charged leptons ($\ell = e, \mu$). A total of 9 data events is observed in good agreement with the background prediction. We set 95% C.L. limits on the $W'WZ$ coupling and on the W' production cross section multiplied by the branching fractions. We also exclude W' masses between 188 and 520 GeV within a simple extension of the standard model and set the most restrictive limits to date on low-scale technicolor models.

PACS numbers: 12.60.Nz, 12.60.Cn, 13.85.Rm, 14.70.Pw

The standard model (SM) of particle physics is widely believed to be a low energy approximation of a more fundamental theory of elementary particles and their interactions. Many extensions of the SM, such as the sequential standard model (SSM) [1], extra dimensions [2], little Higgs [3], and technicolor [4] models, predict new heavy W' resonances decaying to a pair of electroweak W and

Z bosons. Some models [2–4] also offer an alternative to the SM mechanism of electroweak symmetry breaking. Thus, the observation of resonant WZ boson production would not only manifest new physics beyond the SM, but also could yield an insight into the origin of mass.

This Letter describes the first search for a heavy charged boson, referred to as the W' , decaying to W and

Z bosons. The CDF and D0 collaborations have searched for a W' decaying to fermions [5–7]. Current limits exclude W' with masses $\lesssim 1$ TeV at 95% C.L., assuming the SSM as benchmark and that the $W' \rightarrow WZ$ decay is fully suppressed. Thus, our search is complementary to the previous studies.

In technicolor, particles such as ρ_T and a_T have narrow widths and can decay to WZ bosons. The experimental signature of these particles is therefore similar to that of a W' . We will interpret the results of our search within the low scale technicolor model (LSTC), where the masses of ρ_T and a_T are predicted to be below 500 GeV, well within the energy reach of the Tevatron. Since ρ_T and a_T have almost the same mass we refer to them collectively as ρ_T . The branching fraction for $\rho_T \rightarrow WZ$ depends strongly on the relative masses of the technipion, $M(\pi_T)$, and technirho, $M(\rho_T)$. The D0 collaboration searched previously for technicolor in the $W\pi_T \rightarrow W + \text{jets}$ final state [8], which is one of the major decay channels for light technipions. In this Letter we present a search in a previously unexplored region of LSTC phase space with $M(\pi_T) \lesssim M(\rho_T)$ where ρ_T decays predominantly to a WZ boson pair.

We perform the search using data collected with the D0 detector [9] at the Fermilab Tevatron $p\bar{p}$ collider at a center of mass energy of $\sqrt{s} = 1.96$ TeV. After applying data quality and trigger requirements, the integrated luminosity corresponds to 4.1 fb^{-1} .

The Monte Carlo (MC) samples for resonant WZ signal and SM backgrounds are generated using PYTHIA [10], with the exception of $Z + \text{jets}$ and $t\bar{t}$ processes that are generated using ALPGEN [11] interfaced with PYTHIA for showering and hadronization. All MC samples are passed through a full GEANT [12] simulation of the D0 detector. The MC is corrected to describe the luminosity dependence of the trigger and reconstruction efficiencies in data and the contribution from multiple $p\bar{p}$ interactions. The MC sample for signal is produced assuming SSM W' production for masses starting at 180, 190, 200 GeV and then up to 1 TeV in steps of 50 GeV, using CTEQ6L1 [13] parton distribution functions (PDF). The interference between signal and the SM s -channel WZ production [14] is negligible and is not taken into account. We generate technicolor WZ samples typical parametrization of LSTC phenomenology implemented in PYTHIA [15] to estimate the leading order cross section, efficiency, and acceptance of the selection criteria of the $\rho_T \rightarrow WZ$ production. All MC samples are normalized to the integrated luminosity using next-to-leading order cross section calculations, with the exception of the W' signal cross section, which is known to next-to-next-to-leading order (NNLO) [16]. All MC samples are subject to the same event selection as applied to data.

In this search we select events where both the W and the Z bosons decay leptonically and consider only final

states with electrons and muons. Candidate events with at least two final state electrons are selected using single-electron triggers, while those with at least two muons are selected using single-muon triggers resulting in efficiencies of 100% and 92% respectively for signal events. The events are required to have missing transverse energy $\cancel{E}_T > 30$ GeV [17] (from the undetected neutrino) and at least three charged leptons with transverse momenta $p_T > 20$ GeV satisfying the electron or muon identification criteria described below. An electron candidate is identified as a central track matched to an isolated cluster of energy in the calorimeter, with a shower shape consistent with that of an electron, in the pseudorapidity range $|\eta| < 1.1$ or $1.5 < |\eta| < 2.5$. A muon candidate is reconstructed from segments in the muon spectrometer matched to a central track, and is required to be within $|\eta| < 2$. The muon candidate must be isolated from other activity in the tracker and calorimeter.

The selection of WZ candidate events is done in two steps. We first require the presence of a candidate Z boson by selecting the electron pairs and muon pairs with opposite electric charges that have invariant mass nearest to the mass of the Z boson. The reconstructed mass of the Z boson candidate must be between 80 and 102 GeV for an electron pair and between 70 and 110 GeV for a muon pair. Then, we select the highest transverse momentum lepton among the remaining lepton candidates in the event as the lepton from the W boson decay. The W and Z bosons produced from heavy resonances can be highly boosted, resulting in a large spatial separation between leptons from the W and Z decays. To reduce background, we require the lepton from the W boson decay to be separated by $\Delta\mathcal{R} = \sqrt{(\Delta\eta)^2 + (\Delta\phi)^2} > 1.2$ from Z decay leptons.

Several background processes contribute to the trilepton + \cancel{E}_T final state. The largest background having at least three genuine leptons in the final state is from SM WZ production, followed by the ZZ process, where one of the leptons from the Z boson is not reconstructed and gives rise to \cancel{E}_T . These are estimated from MC simulation. The instrumental background is due to misidentification of a lepton in processes such as $Z + \text{jets}$, $Z\gamma$, and $t\bar{t}$. Contribution from $t\bar{t}$ is estimated from MC simulation and found to be negligible. $Z + \text{jets}$ and $Z\gamma$ productions are the major instrumental backgrounds and they are estimated using data driven techniques described below.

Jets from $Z + \text{jets}$ production can be misidentified as either an electron or a muon from W boson decay. To estimate this contribution, we select a sample of Z boson decays with an additional "false" lepton candidate for each final state. For the $Z + \text{electron}$ final state the lepton candidate is required to have most of its energy deposited in the electromagnetic calorimeter and satisfy the electron isolation criteria, but at the same time a shower shape inconsistent with that of an electron. For the $Z + \text{muon}$ final state, the lepton candidate is required

to fail the isolation criteria used to select muons. These requirements ensure that the lepton is either a misidentified jet or a lepton from a semileptonic decay of a heavy-flavor quark. The contribution from the $Z + \text{jets}$ background with misidentified leptons is estimated by scaling the number of events in this sample with a p_T -dependent ratio of misidentified leptons passing the two different sets of criteria measured in a multijet data sample depleted of true isolated leptons.

The channels with $W \rightarrow e\nu$ decays can be mimicked by the initial or final state radiation $Z\gamma$ processes where a photon is either incorrectly matched to a track, or converts, and one of the conversion electrons is selected as the candidate for W boson decay. To estimate the contribution from this background, we measure the rate at which a photon can be misidentified as an electron in $Z \rightarrow \mu\mu\gamma$ final states in data, as it offers a virtually background-free source of photons because of the $\mu\mu\gamma$ invariant mass constraint to the $M(Z)$. We choose the muon decay of the Z boson to avoid ambiguity in assigning the electromagnetic showers in the $ee\gamma$ final states. The $Z\gamma$ contribution is estimated by folding in the p_T -dependent photon to electron misidentification rate with the p_T distribution of γ in the $Z\gamma$ Monte Carlo simulation [18].

The selection criteria yield 9 events in data with an estimate of 10.2 ± 1.6 background events. The final numbers of observed candidates and expected signal and background events with total uncertainties are summarized in Table I. The expected and observed yields for the four independent samples used in this search are given in Table II. Several sources of systematic uncertainties are considered here. The major systematic uncertainty is associated with the modeling of the trigger, the lepton identification efficiency and the detector acceptance. It is estimated to be 15%. This uncertainty is taken as fully correlated between signal and background. We assign to the $Z\gamma$ background estimation a systematic uncertainty of 100% for any potential mis-modeling of \cancel{E}_T . The dominant systematic uncertainty on $Z + \text{jets}$ background is from the limited statistics of the $Z + \text{“false”}$ lepton sample. We estimate this uncertainty to be 40%. Finally, the uncertainty on integrated luminosity is 6.1% [19], and the uncertainty on the theoretical NNLO production cross section of signal is 5%.

As the number of observed candidates is consistent with the background-only hypothesis, we set limits on W' production in a modified frequentist approach [20] that uses a log-likelihood ratio (LLR) test statistic [21]. It calculates the confidence levels for the signal + background, CL_{s+b} , and background-only hypothesis, CL_b , by integrating the LLR distributions obtained from simulated pseudo-experiments using Poisson statistics. Systematic uncertainties are treated as uncertainties on the expected number of signal and background events. This ensures that the uncertainties and their correlations are

Source	Total
$W'(500 \text{ GeV})$	4.4 ± 1.1
WZ	9.0 ± 1.5
ZZ	1.0 ± 0.2
$Z + \text{jets}$	0.2 ± 0.1
$Z\gamma$	0.1 ± 0.1
Total	10.2 ± 1.6
Observed	9

TABLE I: Number of data events, expected number of signal events for a SSM W' mass of 500 GeV and expected number of background events with statistical and systematic uncertainties.

propagated to the outcome with proper weights. The 95% confidence level (C.L.) limit on the cross section is then defined as a cross section for which the ratio $CL_s = CL_{s+b}/CL_b$ is 0.05.

We use the WZ transverse mass to discriminate between the W' signal and the backgrounds in the limit setting procedure. It is calculated as

$$M_T = \sqrt{(E_T^Z + E_T^W)^2 - (p_x^Z + p_x^W)^2 - (p_y^Z + p_y^W)^2},$$

where E_T^Z and E_T^W are the scalar sums of the transverse momenta of the decay products of the Z and W candidates, respectively; while p_x^Z , p_x^W , p_y^Z , and p_y^W are obtained by summing the x and y components of momenta of the respective decay particles. In these sums, the transverse momentum of the neutrino arising from the W boson decay is inferred from the direction and magnitude of \cancel{E}_T . The distribution of the WZ transverse mass is given in Fig. 1 for data, backgrounds, and two signal hypotheses. We obtain a limit on the production cross section of W' multiplied by the branching ratio $B(W' \rightarrow WZ)$ as a function of the $M(W')$ as shown in Fig. 2. This is the first limit to date on resonant $W' \rightarrow WZ$ production. Assuming SSM production, we exclude a W' with mass $188 < M(W') < 520$ GeV at 95% C.L.. This result agrees with the expected sensitivity limit of $188 < M(W') < 497$ GeV.

We also study the sensitivity to other models that predict a W' -like resonance with width greater than in the SSM by varying the width of the W' resonance while keeping $\sigma(W') \times B(W' \rightarrow WZ)$ fixed to the SSM value. We find that the limits slightly degrade but stay within 1 standard deviation (s.d.) around the expected sensitivity limits for models with widths up to 25% of the resonance mass. Since the limits have a limited sensitivity to the width of the W' , we can exclude more general models that predict W' bosons with arbitrary couplings to the W and Z bosons. We interpret the results in terms of the $W'WZ$ trilinear coupling normalized to the SSM value as function of the W' mass (see Fig. 3).

The limits on the resonant WZ production cross section $\sigma \times B(W' \rightarrow WZ)$ yield stringent constraints on

Mode	WZ	ZZ	$Z + \text{jets}$	$Z\gamma$	Total	W'	Data
eee	1.4 ± 0.3	0.07 ± 0.02	0.02 ± 0.01	0.03 ± 0.03	1.52 ± 0.33	1.07 ± 0.28	3
$ee\mu$	2.0 ± 0.4	0.24 ± 0.06	0.07 ± 0.04	< 0.01	2.31 ± 0.49	1.17 ± 0.31	2
$e\mu\mu$	2.0 ± 0.4	0.10 ± 0.03	0.04 ± 0.02	0.07 ± 0.07	2.21 ± 0.46	0.83 ± 0.22	2
$\mu\mu\mu$	3.6 ± 0.8	0.54 ± 0.12	0.05 ± 0.03	< 0.01	4.19 ± 0.89	1.28 ± 0.34	2

TABLE II: Background estimation from the leading sources, the total background, expected signal, and observed events for each signature. The signal corresponds to a SSM W' with a mass of 500 GeV. The uncertainties reflect both the statistics of the MC and data samples and systematics.

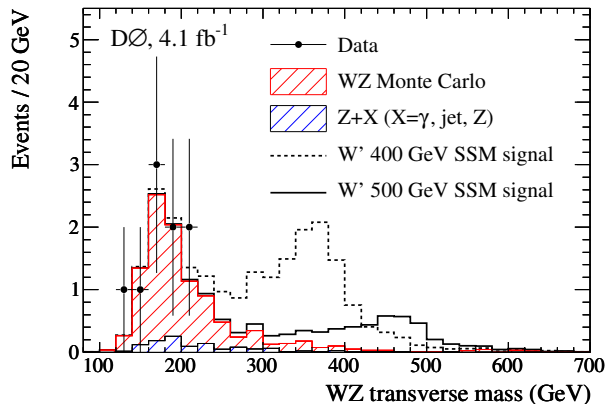


FIG. 1: Transverse mass distribution of the WZ system in data with the major SM backgrounds and two SSM W' mass hypotheses overlaid (color online).

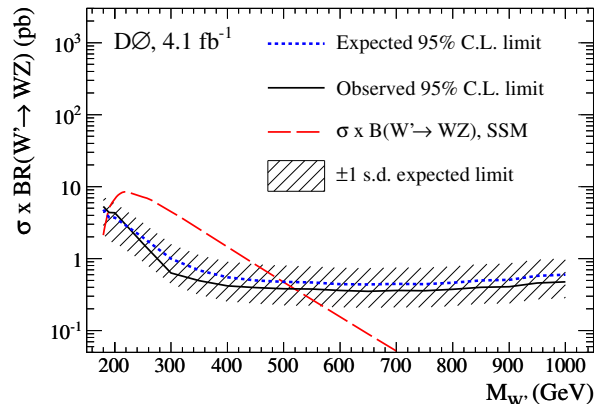


FIG. 2: Observed and expected 95% C.L. upper limits and ± 1 s.d. band around the expected limits on the cross section multiplied by $B(W' \rightarrow WZ)$ with the SSM prediction overlaid (color online).

the LSTC and exclude most of the allowed phase space where $\rho_T \rightarrow WZ$ decay is dominant. The excluded and expected limits at 95% C.L., as a function of the ρ_T and π_T masses, are shown in Fig. 4.

In summary, we have presented a search for hypothetical W' particles decaying to a pair of WZ bosons using leptonic W and Z decay modes in 4.1 fb^{-1} of Tevatron Run II data. We observe no evidence of resonant WZ production, and set limits on the production cross section $\sigma \times B(W' \rightarrow WZ)$. Within the SSM we exclude W' masses between 188 and 520 GeV at 95% C.L. This is the best limit to date on $W' \rightarrow WZ$ production and is complementary to previous searches [5–7] for W' decay to fermions. These limits are less stringent for the models that predict W' with width greater than that predicted by the SSM model, but stay within the 1 s.d. band around the expected SSM limits for widths below 25% of the W' mass. The original limits are also interpreted within the technicolor model. We exclude ρ_T with mass between 208 and 408 GeV at 95% C.L. for $M(\rho_T) < M(\pi_T) + M(W)$. These are the most stringent constraints on the LSTC phenomenology model [15] when the ρ_T decays predominantly to WZ boson pair.

We thank Kenneth Lane for useful discussions and help with interpretation of the results within the TCSM parameter space and we thank the staffs at Fermilab

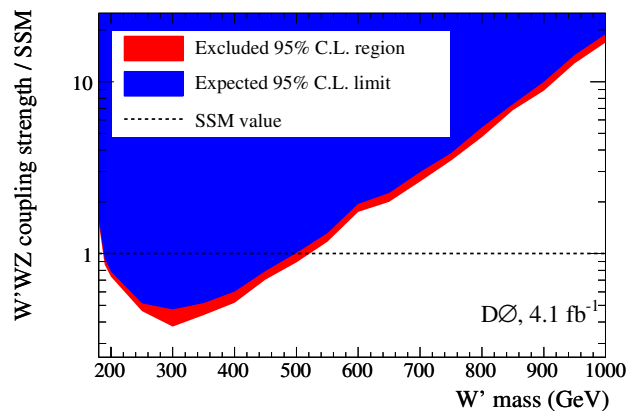


FIG. 3: Expected and excluded area of the $W'WZ$ coupling strength normalized to the SSM value as a function of the W' mass (color online).

and collaborating institutions, and acknowledge support from the DOE and NSF (USA); CEA and CNRS/IN2P3 (France); FASI, Rosatom and RFBR (Russia); CNPq, FAPERJ, FAPESP and FUNDUNESP (Brazil); DAE and DST (India); Colciencias (Colombia); CONACyT (Mexico); KRF and KOSEF (Korea); CONICET and

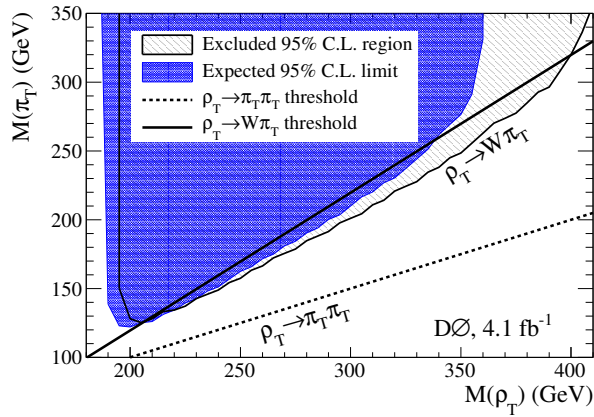


FIG. 4: Expected and excluded areas of the π_T vs. ρ_T masses are given with the thresholds of the $\rho_T \rightarrow W\pi_T$ and $\rho_T \rightarrow \pi_T\pi_T$ overlaid (color online).

UBACyT (Argentina); FOM (The Netherlands); STFC and the Royal Society (United Kingdom); MSMT and GACR (Czech Republic); CRC Program, CFI, NSERC and WestGrid Project (Canada); BMBF and DFG (Germany); SFI (Ireland); The Swedish Research Council (Sweden); CAS and CNSF (China); and the Alexander von Humboldt Foundation (Germany).

-
- [a] Visitor from Augustana College, Sioux Falls, SD, USA.
[b] Visitor from Rutgers University, Piscataway, NJ, USA.
[c] Visitor from The University of Liverpool, Liverpool, UK.
[d] Visitor from SLAC, Menlo Park, CA, USA.
[e] Visitor from Centro de Investigacion en Computacion - IPN, Mexico City, Mexico.
[f] Visitor from ECFM, Universidad Autonoma de Sinaloa, Culiacán, Mexico.
[g] Visitor from Universität Bern, Bern, Switzerland.
[h] Visitor from Universität Zürich, Zürich, Switzerland.

- [1] J.C. Pati, A. Salam, Phys. Rev. D **10**, 275 (1974) [Erratum-ibid. D **11**, 703 (1975)]; G. Altarelli, B. Mele, M. Ruiz-Altaba, Z. Phys. C **45**, 109 (1989) [Erratum-ibid C **47**, 676 (1990)]; P. Langacker, arXiv:0801.1345 [hep-ph] (2008), and references therein.
[2] H. He *et al.*, Phys. Rev. D **78**, 031701 (2008); A. Belyaev, arXiv:0711.1919 [hep-ph]; K. Agashe *et al.*, Phys. Rev. D **80**, 075007, 2009.
[3] M. Perelstein, Prog. Part. Nucl. Phys. **58**, 247 (2007).
[4] E. Eichten and K. Lane, Phys. Lett. B **669**, 235 (2008); K. Lane, Phys. Rev. D **60**, 075007 (1999).
[5] D. Acosta *et al.*, Phys. Rev. Lett. **90**, 081802 (2003).
[6] A. Abulencia *et al.*, Phys. Rev. D **75**, 091101 (2007).
[7] V. M. Abazov *et al.*, Phys. Rev. Lett. **100**, 211803 (2008).
[8] V. M. Abazov *et al.*, Phys. Rev. Lett. **98**, 221801 (2007).
[9] V.M. Abazov *et al.*, Nucl. Instrum. Methods Phys. Res. A **565**, 463 (2006).
[10] T. Sjöstrand, S. Mrenna, and P. Skands, J. High Energy Phys. **05**, 026 (2006); we used 6.419.
[11] M. L. Mangano *et al.*, J. High Energy Phys. **07**, 1 (2003).
[12] GEANT Detector Description and Simulation Tool, CERN Program Library Long Writup W5013.
[13] J. Pumplin *et al.*, J. High Energy Phys. **0207**, 012 (2002).
[14] T. Rizzo, J. High Energy Phys. **0705**, 037 (2007).
[15] K. Lane and S. Mrenna, Phys. Rev. D **67**, 115011 (2003).
[16] R. Hamburg, W.L. van Neerven and T. Matsuura, Nucl. Phys. B **359**, 343 (1991); Erratum-ibid. B **644**, 403 (2002).
[17] The D0 detector utilizes a right-handed coordinate system with the z axis pointing in the direction of the proton beam and the y axis pointing upwards. The azimuthal angle ϕ is defined in the xy plane measured from the x axis. The pseudorapidity is defined as $\eta = -\ln[\tan(\theta/2)]$, where $\theta = \arctan(\sqrt{x^2 + y^2}/z)$. The transverse variables are defined as projections of the variables onto the $x - y$ plane. The missing transverse energy is the imbalance of the momentum estimated from the calorimeter and reconstructed muons in the $x - y$ plane.
[18] U. Baur and E. Berger, Phys. Rev. D **47**, 4889 (1993).
[19] T. Andeen *et al.*, FERMILAB-TM-2365 (2007).
[20] W. Fisher, FERMILAB-TM-2386-E.
[21] T. Junk, Nucl. Instrum. Methods Phys. Res. A **434**, 435 (1999); A. Read, CERN 2000-005 (2000).